

## RESEARCH ARTICLE

10.1029/2017JD028181

## Key Points:

- Fossil fuel contribution of precipitation WSOC at Nam Co station in the inland Tibetan Plateau was around  $15 \pm 6\%$
- Precipitation WSOC was depleted in dissolved black carbon and sulfurous organic molecules at Nam Co station
- Fossil-derived precipitation WSOC at Nam Co station was mainly transported from South Asia

## Supporting Information:

- Supporting Information S1

## Correspondence to:

C. Li, S. Kang and A. Stubbins,  
lichao.li@itpcas.ac.cn;  
shichang.kang@lzb.ac.cn;  
a.stubbins@northeastern.edu

## Citation:

Li, C., Chen, P., Kang, S., Yan, F., Tripathi, L., Wu, G., et al. (2018). Fossil fuel combustion emission from South Asia influences precipitation dissolved organic carbon reaching the remote Tibetan Plateau: Isotopic and molecular evidence. *Journal of Geophysical Research: Atmospheres*, 123, 6248–6258. <https://doi.org/10.1029/2017JD028181>

Received 9 DEC 2017

Accepted 11 MAY 2018

Accepted article online 18 MAY 2018

Published online 4 JUN 2018

# Fossil Fuel Combustion Emission From South Asia Influences Precipitation Dissolved Organic Carbon Reaching the Remote Tibetan Plateau: Isotopic and Molecular Evidence

Chaoliu Li<sup>1,2,3</sup> , Pengfei Chen<sup>4</sup>, Shichang Kang<sup>4,2,5</sup> , Fangping Yan<sup>3</sup>, Lekhendri Tripathi<sup>4</sup>, Guangjian Wu<sup>1,2</sup> , Bin Qu<sup>6</sup>, Mika Sillanpää<sup>3</sup>, Di Yang<sup>7</sup>, Thorsten Dittmar<sup>8</sup> , Aron Stubbins<sup>9</sup> , and Peter A. Raymond<sup>10</sup> 

<sup>1</sup>Key Laboratory of Tibetan Environment Changes and Land Surface Processes, Institute of Tibetan Plateau Research, Chinese Academy of Sciences, Beijing, China, <sup>2</sup>CAS Center for Excellence in Tibetan Plateau Earth Sciences, Beijing, China, <sup>3</sup>Laboratory of Green Chemistry, Lappeenranta University of Technology, Mikkeli, Finland, <sup>4</sup>State Key Laboratory of Cryospheric Science, Northwest Institute of Eco-Environment and Resources, Chinese Academy of Sciences, Lanzhou, China, <sup>5</sup>University of CAS, Beijing, China, <sup>6</sup>Yale-NUIST Center on Atmospheric Environment, International Joint Laboratory on Climate and Environment Change, Nanjing University of Information Science and Technology, Nanjing, China, <sup>7</sup>State Key Laboratory of Oil and Gas Reservoir Geology and Exploitation, Chengdu University of Technology, Chengdu, China, <sup>8</sup>Research Group for Marine Geochemistry (ICBM-MPI Bridging group), Institute for Chemistry and Biology of the Marine Environment, Carl von Ossietzky University of Oldenburg, Oldenburg, Germany, <sup>9</sup>Departments of Marine and Environmental Sciences, Civil and Environmental Engineering, and Chemistry and Chemical Biology, Northeastern University, Boston, MA, USA, <sup>10</sup>School of Forestry and Environmental Studies, Yale University, New Haven, CT, USA

**Abstract** The dissolved organic carbon in precipitation (water-soluble organic carbon, WSOC) can provide a carbon subsidy to receiving ecosystems. The concentrations, isotopic signatures ( $\delta^{13}\text{C}/\Delta^{14}\text{C}$ ), and molecular signatures (transform ion cyclotron mass spectrometry) of WSOC being delivered to Nam Co—a remote site on the inland Tibetan Plateau (TP)—were compared to those of WSOC in the snowpack, and in wet deposition from urban cities fringing the TP. The average WSOC concentration at Nam Co ( $1.0 \pm 0.9 \text{ mg C L}^{-1}$ ) was lower than for the large cities ( $1.6$  to  $2.3 \text{ mg C L}^{-1}$ ) but higher than in the snowpack samples ( $0.26 \pm 0.09 \text{ mg C L}^{-1}$ ). Based upon radiocarbon data, it is estimated that  $15 \pm 6\%$  of Nam Co WSOC was fossil derived, increasing to  $20 \pm 8\%$  for snowpack WSOC,  $29 \pm 4\%$  for Lhasa WSOC, and  $34 \pm 8\%$  for the three cities. Transform ion cyclotron mass spectrometry results revealed that the abundance of dissolved black carbon and sulfur-containing molecules of WSOC increased in the order Nam Co < snow pack < urban. The enrichment in  $^{14}\text{C}$  and depletion in dissolved black carbon and sulfurous organic molecules of Nam Co WSOC was suggestive of low, but still detectable inputs of fossil-derived organics to WSOC on the remote TP. Backward air mass trajectories for the precipitation events at Nam Co suggested that the fossil fuel contributions to WSOC in Nam Co region originated mainly from South Asia. This study provides novel radiocarbon age, chemistry, and source evidence that anthropogenic WSOC is delivered to the remote TP, one of the most remote regions on Earth.

## 1. Introduction

The dissolved organic carbon (DOC) delivered to the land in precipitation (water-soluble organic carbon, WSOC) is derived from many sources including primary emissions, secondary organic aerosols from various gaseous precursors, and gases (Legrand et al., 2007; May et al., 2013). WSOC has an important influence on climate and provides a biolabile carbon subsidy to receiving aquatic ecosystems (Mladenov, Alados-Arboledas, et al., 2011; Mladenov et al., 2008; Mladenov, Sommaruga, et al., 2011; Raymond, 2005; Spencer et al., 2014; Stubbins et al., 2012; Willey et al., 2000; Yang et al., 2003). The organic carbon stripped from the atmosphere and deposited as WSOC derives from multiple sources, including biogenic, wildfires, wind-blown dust, biomass burning, and fossil fuel burning (Hood et al., 2015; Legrand et al., 2013; May et al., 2013; Willey et al., 2000). At present, the original sources of WSOC remain poorly constrained compared to other carbonaceous aerosol species (May et al., 2013).

Radiocarbon isotopic composition ( $\Delta^{14}\text{C}$ ) provides information about the apparent bulk age of WSOC and has been used to estimate fossil contributions to WSOC (Avery et al., 2006, 2013; Graven, 2015; Gustafsson

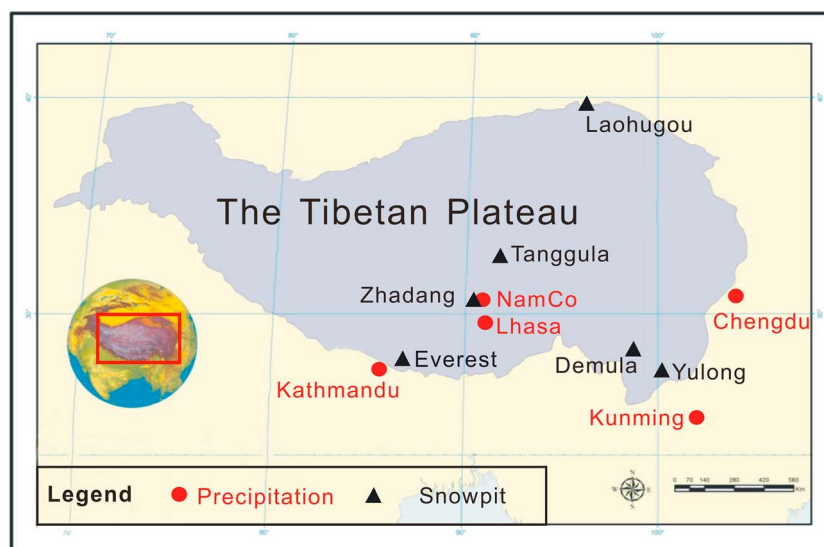


**Figure 1.** Map of the study sites on and around the Tibetan Plateau.

et al., 2009; May et al., 2013; Raymond, 2005; Zencak et al., 2007). The relative abundance of the natural  $^{13}\text{C}$  isotope ( $\delta^{13}\text{C}$ ) provides information about the source and processing of organics (Narukawa et al., 1999). So far, a number of techniques have been developed for investigating structures of WSOC (Decesari et al., 2000; Duarte & Duarte, 2011; Duarte et al., 2007). Ultrahigh-resolution Fourier transform ion cyclotron mass spectrometry (FT-ICR MS) can resolve the molecular formulas present within WSOC (Mopper et al., 2007; Wozniak, Bauer, Sleighter, & Dickhut, 2008).

The Tibetan Plateau (TP) is one of the highest plateaus and most remote areas in the world. However, it is bordered by heavily polluted South and East Asia, and pollutants emitted from these two regions can penetrate into the TP, influencing its atmosphere (Kang et al., 2016; C. Li, Bosch, et al., 2016; Luthi et al., 2015; Xu et al., 2013) and producing serious environmental consequences, including a warming atmosphere and glacier retreat (Ji et al., 2015; X. Li, Kang, et al., 2017; Qian et al., 2011; Ramanathan & Carmichael, 2008; Y. Zhang et al., 2017). A study of glacier ice and glacier-fed streams on the TP inferred that the radiocarbon-depleted DOC found in these systems is a result of the atmospheric deposition of pre-aged, possibly fossil fuel-derived organics (Spencer et al., 2014). However, at present, no study has evaluated fossil fuel contributions to WSOC deposited directly to the TP.

In the current study, we assessed the potential sources of WSOC delivered to the TP for both precipitation and snowpack samples. Precipitation samples were collected from Nam Co Monitoring and Research Station for Multisphere Interactions (Nam Co Station), a site on the TP that is remote from industrial regions (Li et al., 2007; Luthi et al., 2015). WSOC samples from four cities within and around the TP and six snowpack samples were also collected. Samples were analyzed to determine the concentrations, isotopic values ( $\delta^{13}\text{C}/\Delta^{14}\text{C}$ ), and molecular signatures (FT-ICR MS) of WSOC. Nam Co precipitation samples were also analyzed for  $\text{Ca}^{2+}$ ,  $\text{NO}_3^-$ , and  $\text{Na}^+$ , and air mass paths were investigated to assist in ascribing potential geographic source regions for WSOC. The  $\delta^{13}\text{C}$  signatures of river water WSOC and soil organic matter were also determined to assist in constraining the potential sources of WSOC at Nam Co.

## 2. Sampling and Analyses

### 2.1. Sample Sites

Precipitation samples were collected from Nam Co, Lhasa, Chengdu, Kunming, and Kathmandu (Figure 1). Both Chengdu and Kunming are typical large Chinese cities. Kathmandu is the capital city of Nepal and has significant air pollution (P. Chen et al., 2015). Lhasa is the largest and the most popular tourist city of the Tibet Autonomous Region, China. Although the air quality in Lhasa is considered clean when compared to other Chinese cities, its atmosphere is being seriously influenced by local emissions (Huang et al., 2010;

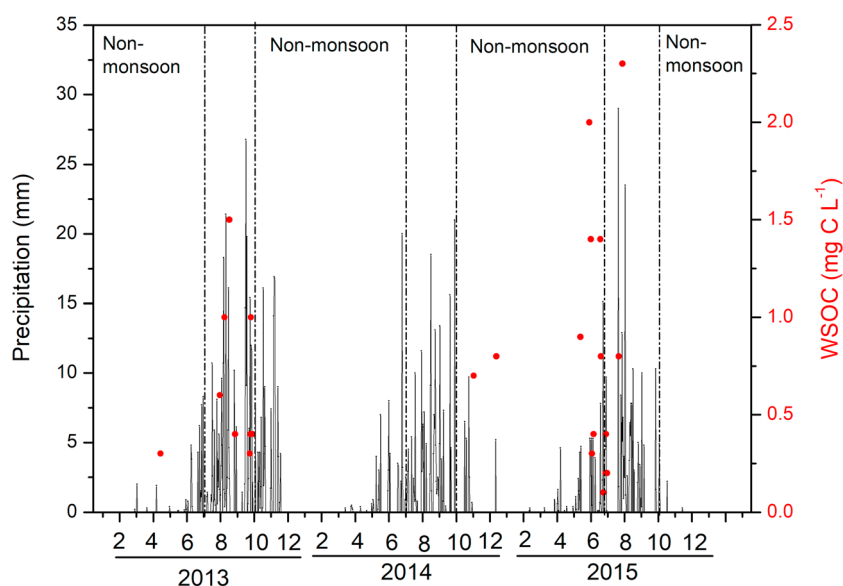


**Figure 2.** Seasonal variations in precipitation and water-soluble organic carbon (WSOC) at Nam Co station from 2013 to 2015.

C. Li, Bosch, et al., 2016). Nam Co ( $30^{\circ}46'N$ ,  $90^{\circ}59'E$ , 4,700 m above sea level) is a sparsely populated, remote, high-elevation region on the TP with minimal local anthropogenic aerosols sources. Its climate can be divided into nonmonsoon from October to May and monsoon from June to September. Most precipitation occur during monsoon period (Figure 2). Glaciers cover a large area of the TP and are far from anthropogenic emission centers (C. Li, Chen, Kang, Yan, Li, et al., 2016).

## 2.2. Sampling Methods

Sampling for WSOC from precipitation and snowpack samples followed established methods (C. Li, Chen, Kang, Yan, Li, et al., 2016; C. Li, Yan, Kang, Chen, Hu, et al., 2017; C. Li, Yan, Kang, Chen, Qu, et al., 2016), which are presented in the supporting information (S1). A total of 29 precipitation samples was collected at Nam Co from 2013 to 2015. Seven samples were analyzed for WSOC and  $\delta^{13}C/\Delta^{14}C$ , and three via FT-ICR MS. A total of 14 other WSOC samples from four cities located at the fringe of the TP (Kunming,  $n = 3$ ; Chengdu,  $n = 3$ ; Kathmandu,  $n = 5$ ; Lhasa,  $n = 3$ ) was analyzed for WSOC and  $\delta^{13}C/\Delta^{14}C$ . Four of these samples were analyzed via FT-ICR MS (Kunming,  $n = 2$ ; Chengdu,  $n = 1$ ; Kathmandu,  $n = 1$ ; Lhasa,  $n = 0$ ). Ten snowpack samples were analyzed for WSOC and  $\delta^{13}C/\Delta^{14}C$ , eight via FT-ICR MS. In addition,  $\delta^{13}C$  values were determined for 14 surface soil organic matter samples of the TP based on the protocol from Lu et al. (2004).

## 2.3. WSOC and Ion Concentrations

WSOC samples were filtered through prebaked glass filters (Whatman GF/F, pore size  $0.7\ \mu m$ , diameter 47 mm) to remove particles. WSOC was quantified using a high-temperature oxidation method (TOC-5000A; Shimadzu Corp, Kyoto, Japan; Stubbins & Dittmar, 2012). WSOC concentrations of the process blanks ( $0.04 \pm 0.02\ mg\ C\ L^{-1}$ ,  $n = 8$ ) were similar to our previous results (F. Yan et al., 2016) and much lower than those of samples.  $Ca^{2+}$ ,  $NO_3^-$ , and  $Na^+$  were measured by ion chromatography (Dionex ISC 2000/2500, United States; Li et al., 2007). The average blank concentrations of measured ions were low of less than 1 ng/g. All the reported concentrations were subtracted by those of the blanks.

## 2.4. WSOC Isotopic Analysis

For  $\delta^{13}C/\Delta^{14}C$  analysis, WSOC samples were shipped frozen to the United States, oxidized to  $CO_2$  using ultraviolet light and purified at the Yale School of Forestry and Environmental Studies following published methods (Raymond et al., 2004, 2007). Briefly, for samples containing more than  $60\ \mu g\ C$ , sample was poured into precleaned quartz tubes, acidified to pH 2 with phosphoric acid, and sparged with ultrahigh purity helium to remove inorganic carbon. Next, the sample was irradiated using a high-energy ultraviolet lamp

for 5 hr to quantitatively oxidize WSOC to CO<sub>2</sub>. Concentrations of WSOC were determined using a calibrated Baratron absolute pressure gauge (MKS Industries). WSOC concentrations determined agree well with those determined using the Shimadzu TOC analyzer described above ( $r^2 = 0.99$ , slope = 1.03; Figure S1) and as previously reported in this laboratory (Raymond et al., 2007). CO<sub>2</sub> was cryogenically purified by liquid nitrogen on a vacuum extraction line and sent to the National Ocean Sciences Accelerator Mass Spectrometry at Woods Hole for isotopic analysis. Recoveries and blanks were assessed periodically by oxidizing a dissolved organic standard (oxalic acid) using the same procedure as for samples.  $\Delta^{14}\text{C}$  of the standard agreed well with reference values. CO<sub>2</sub> produced for the procedural blanks was insufficient for radiocarbon analyses. A binary mixing model was used to obtain fractional contributions of contemporary biogenic ( $f_{\text{biogenic}}$ ) and fossil ( $f_{\text{fossil}} = 1 - f_{\text{biogenic}}$ ) derived organics to the WSOC of the measured samples (Kirillova et al., 2013). This mixing model is described further in the supporting information (Text S3).

### 2.5. Fourier Transform Ion Cyclotron Resonance Mass Spectrometry

In order to concentrate and purify WSOC for FT-ICR MS analysis, samples were solid phase extracted using PPL Bond Elut (Agilent) resins. Samples were acidified to pH 2 using ultrapure hydrochloric acid and solid phase extracted following the method of Dittmar et al. (2008). The methanol extracts were diluted 1:1 with ultrapure water and analyzed in negative mode electrospray ionization using a 15 Tesla FT-ICR MS (Bruker Solarix) at the University of Oldenburg, Germany. Five hundred broadband scans were accumulated for the mass spectra. After internal calibration, mass accuracies were within an error of <0.2 ppm. Molecular formulas were assigned to peaks with signal-to-noise ratios greater than 5 based on published rules (Koch et al., 2007; Singer et al., 2012; Stubbins et al., 2010). Peaks detected in the procedural blank (PPL extracted ultrapure water) were removed. Peak detection limits were standardized between samples by adjusting the dynamic range of each sample to that of the sample with the lowest dynamic range (dynamic range = average of the largest 20% of peaks assigned a formula divided by the signal-to-noise threshold intensity; standardized detection limit = average of largest 20% of peaks assigned a formula within a sample divided by the lowest dynamic range within the sample set; Spencer et al., 2014; Stubbins et al., 2014). Peaks below the standardized detection limit were removed to prevent false negatives for the occurrence of a formula within samples with low dynamic range.

Assigned formulas were categorized by compound class based upon elemental stoichiometries (Stubbins et al., 2010). Modified aromaticity index (Almod) (Koch & Dittmar, 2006) values were calculated:

$$\text{Almod} = (1 + \text{C} - 0.5\text{O} - \text{S} - 0.5\text{H}) / (\text{C} - 0.5\text{O} - \text{S} - \text{N} - \text{P}) \quad (1)$$

Formulas with Almod values from 0.5 to 0.67 were assigned as aromatic, and formulas with Almod greater than 0.67 were assigned as dissolved black carbon (Koch & Dittmar, 2006). As such, the term dissolved black carbon is used here to denote soluble forms of combustion-derived condensed aromatic compounds (Kim et al., 2004; Stubbins et al., 2010). The further compound classes were defined as follows: highly unsaturated = Almod < 0.5, H/C < 1.5; aliphatics = H/C 1.5 to 2.0, O/C < 0.9, N = 0; peptide molecular formulas = H/C 1.5 to 2.0, O/C < 0.9, and N > 0. It should be noted that compounds identified as "peptides" have the molecular formulas of peptides, but their actual structure may differ. Elemental formulas were also grouped by elemental composition (i.e., without N, S, or P = CHO only; with S, with N, and with P).

### 2.6. Air Mass Trajectories

In order to investigate air mass source for a given precipitation event over Nam Co, 5-day backward trajectories (100, 500, and 1,000 m above ground level, AGL) were achieved using the Hybrid Single-Particle Lagrangian Integrated Trajectory 4 model developed by National Oceanic and Atmospheric Administration (<http://www.arl.noaa.gov/ready/hysplit4.html>; Rolph, 2015).

## 3. Results

### 3.1. Calcium and Nitrate

Ca<sup>2+</sup> in Nam Co precipitation ranged from 3 to 4,990  $\mu\text{g/L}$ . NO<sub>3</sub><sup>-</sup> in Nam Co precipitation ranged from 72 to 1,860  $\mu\text{g/L}$  (Table S1).

**Table 1**

Average WSOC Concentrations,  $\delta^{13}\text{C}$  Signatures, Fossil Contribution ( $f_{\text{fossil}}$ ), and Apparent Age ( $^{14}\text{C}$  Age) in ybp, and Percentage DBC and Sulfurous (With Sulfur) Compounds Based Upon Fourier Transform Ion Cyclotron Resonance Mass Spectrometry Data for Snowpack and WSOC Samples

Sampling site	WSOC ( $\text{mg C L}^{-1}$ )	$\delta^{13}\text{C}$ (‰)	$f_{\text{fossil}}$ (%)	$^{14}\text{C}$ age (ybp)	DBC (%)	Sulfur (%)
Snowpack	$0.26 \pm 0.09$	$-21 \pm 3$	$20 \pm 8$	$1300 \pm 570$	$1.7 \pm 0.6$	$13 \pm 8$
Nam Co	$1.0 \pm 0.9$	$-21 \pm 3$	$15 \pm 6$	$1080 \pm 530$	$0.6 \pm 0.5$	$3 \pm 2$
Lhasa	$1.0 \pm 0.4$	$-25 \pm 2$	$29 \pm 4$	$1750 \pm 460$	N.D.	N.D.
Chengdu	$2.3 \pm 0.4$	$-24.2 \pm 0.2$	$33 \pm 9$	$2300 \pm 1100$	$2.6 \pm 0.6$	$31 \pm 13$
Kunming	$1.6 \pm 1.2$	$-26 \pm 2.0$	$36 \pm 10$	$2600 \pm 1200$	$3.9 \pm 0.6$	$35 \pm 29$
Kathmandu	$1.7 \pm 1.2$	$-25.2 \pm 0.8$	$33 \pm 9$	$2200 \pm 1100$	1.7	3.9

Note. WSOC = water-soluble organic carbon; ybp = years before present; DBC = dissolved black carbon; N.D. = no data.

### 3.2. WSOC Concentration

The snowpack samples had the lowest average WSOC concentration ( $0.26 \pm 0.09 \text{ mg C L}^{-1}$ ). The mean concentration of WSOC at Nam Co ( $1.0 \pm 0.9 \text{ mg C L}^{-1}$ ) was lower than the three other cities (1.6 to  $2.3 \text{ mg C L}^{-1}$ ; Figure S2a and Table 1).

### 3.3. Isotopic Signatures of WSOC

$\delta^{13}\text{C}$  values (Figure S2b and Table 1) of snowpack WSOC ( $-21 \pm 3\text{‰}$ ) and Nam Co WSOC ( $-21 \pm 3\text{‰}$ ) were variable and enriched compared to WSOC from Lhasa ( $-25 \pm 3\text{‰}$ ) and other cities ( $-24$  to  $-26\text{‰}$ ).  $\delta^{13}\text{C}$  values for WSOC of Nam Co and snowpack were also enriched relative to soil organic carbon ( $\delta^{13}\text{C} = -25.4 \pm 0.6\text{‰}$ ) and river water WSOC ( $\delta^{13}\text{C} = -25.6 \pm 1.24\text{‰}$ ) from the TP (Figure 3 and Table S3).

Nam Co WSOC ( $1080 \pm 530$  years before present, ybp) and snowpack WSOC ( $1300 \pm 570$  ybp) samples had the youngest apparent radiocarbon ages (Figure S2c and Table 1). WSOC from the three large cities fringing the TP was most depleted in  $^{14}\text{C}$  resulting in the oldest average apparent radiocarbon ages (2200 to 2600 ybp). Lhasa WSOC was of intermediate radiocarbon age ( $1750 \pm 460$  ybp).

### 3.4. Molecular Signatures of Snowpack and WSOC

Molecular formulas covered a wide range of H/C and O/C values (Figure 4) and molecular classes (Tables 1 and S4). Nam Co WSOC was depleted in dissolved black carbon and sulfur-containing formulas relative to WSOC from the cities and snowpack (Figures S2d, S2e, and 4 and Tables 1 and S4). WSOC from the large cities had the highest and most variable proportions of dissolved black carbon and sulfur-containing formulas (Figures S2d, S2e, and 4 and Tables 1 and S4).

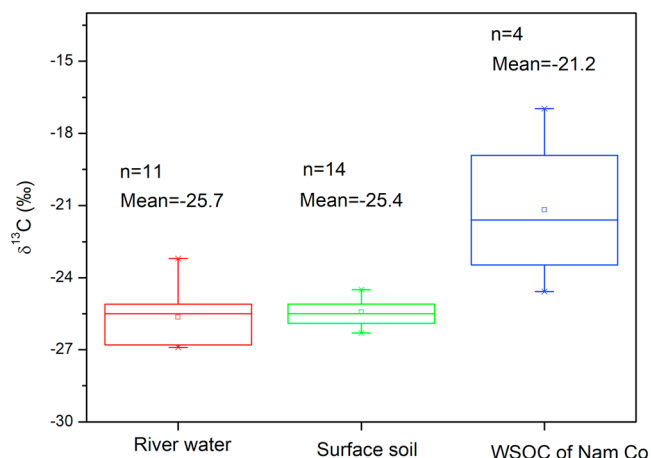


**Figure 3.**  $\delta^{13}\text{C}$  of Nam Co water-soluble organic carbon (WSOC), organic carbon from the surface soil, and river water WSOC from the Tibetan Plateau.

## 4. Discussion

### 4.1. Concentrations of WSOC

WSOC concentrations in samples collected at the large cities were highly variable and elevated compared to Lhasa and Nam Co WSOC (C. Li, Yan, Kang, Chen, Hu, et al., 2017; C. Li, Yan, Kang, Chen, Qu, et al., 2016; Figure S2a and Table 1). High city WSOC concentrations were comparable to WSOC concentrations for samples collected in other large Asian cities such as Beijing, China ( $3.50 \text{ mg C L}^{-1}$ ; Pan et al., 2010) and Seoul, South Korea ( $1.13 \text{ mg C L}^{-1}$ ; G. Yan & Kim, 2012). Average concentrations of Nam Co WSOC were lower than urban WSOC concentrations but higher than snowpack WSOC concentrations (Table 1 and Figure S2a). The low concentrations of snowpack WSOC on the TP are in agreement with previous studies in Alaska (Fellman et al., 2015), Antarctica (Antony et al., 2014; Barker et al., 2013), the European Alps (Legrand et al., 2013), and Greenland (Grannas et al., 2004; Twickler et al., 1986). Given the photolability (Grannas et al., 2004) and biolability (Hood et al., 2009; Spencer et al., 2014) of WSOC



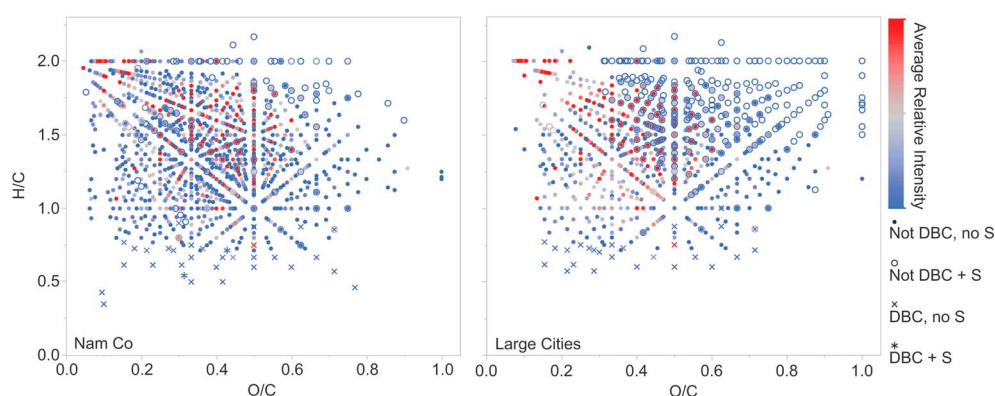


**Figure 4.** Van Krevelen diagrams displaying the average molecular properties of water-soluble organic carbon for samples collected from Nam Co and the large cities. DBC = dissolved black carbon; S = sulfur.

found in accumulating snow and exported from glaciers, it is likely that a fraction of WSOC is lost to biodegradation or photodegradation once deposited as snow and this results in WSOC concentrations being lower in snowpacks than in the precipitation that forms snowpacks.

#### 4.2. Sources of WSOC

The WSOC samples from Lhasa and the three large cities were depleted in  $^{14}\text{C}$ , equating to older apparent ages, relative to WSOC at Nam Co, the remote site on the TP (Figure S2c and Table 1). The FT-ICR MS data also showed the WSOC samples from the large cities to be enriched in dissolved black carbon and sulfurous compounds relative to Nam Co WSOC (Figures S2d and S2e and Table 1). Dissolved black carbon and sulfurous compounds are both molecular signatures associated with combustion products (Wozniak, Bauer, Sleighter, Dickhut, & Hatcher, 2008). Therefore, the depletion in  $^{14}\text{C}$  and enrichment in dissolved black carbon and sulfurous compounds in WSOC from the large cities suggests that urban precipitation is enriched in WSOC due to the high level of anthropogenic emissions and associated fossil fuel combustion in these regions (B. Chen et al., 2013; Y.-L. Zhang, Huang, et al., 2015). Based upon a binary isotopic mass balance percentage contribution of fossil fuel-derived organics to total WSOC was  $29 \pm 4\%$  at Lhasa, increasing for the three large cities (Kunming =  $36 \pm 10\%$ ; Chengdu =  $34 \pm 9\%$ ; Kathmandu =  $33 \pm 10\%$ ; Table 1). These values are comparable to those for WSOC samples from an urban area in North America ( $27 \pm 20\%$ ; Raymond, 2005) and slightly higher than that of WSOC of near-surface aerosols in western India ( $23 \pm 4\%$ ; Kirillova et al., 2013).

Nam Co WSOC was enriched in  $^{14}\text{C}$  and depleted in dissolved black carbon and sulfurous compounds relative to the urban sites (Figure S2 and Table 1), suggesting that the low concentration of WSOC at Nam Co reflects the weaker influence of human activity at this high-elevation, remote region (Li et al., 2007). Despite the lower apparent input of anthropogenic carbon in Nam Co WSOC,  $f_{\text{fossil}}$  of Nam Co WSOC samples averaged  $15 \pm 6\%$ , indicating that around one seventh of WSOC in this remote region could be derived from fossil fuel combustion. As there are no to minimal fossil fuel combustion emissions at Nam Co, this fossil fuel-derived organic carbon would have to originate from emission sites distant from Nam Co. Additional data and discussion is presented below to further qualify the assumption that the  $^{14}\text{C}$  depleted component of Nam Co WSOC was derived from distant fossil fuel combustion.

Surface soils may contain aged organic carbon, which can be entrained into the atmosphere as dust and incorporated into WSOC. Therefore, dust from local soils on the TP could contribute  $^{14}\text{C}$  depleted carbon to Nam Co WSOC.  $\text{Ca}^{2+}$  and  $\text{NO}_3^-$  in precipitation at Nam Co derive from soil/dust and combustion, respectively (Li et al., 2007; Liu et al., 2015). Nam Co WSOC concentrations correlated linearly with  $\text{NO}_3^-$  concentrations ( $R^2 = 0.79$ ;  $p < 0.0001$ ;  $n = 27$ ), but not non-sea-salt  $\text{Ca}^{2+}$  (Drever, 1982;  $R^2 = 0.03$ ;  $p = 0.37$ ;  $n = 27$ ; Figure S3; Pulido-Villena et al., 2006). These trends in WSOC,  $\text{NO}_3^-$  and non-sea-salt  $\text{Ca}^{2+}$  suggest that WSOC at Nam Co is mainly derived from combustion, not soils (C. Li, Yan, Kang, Chen, Hu, et al., 2017). It needs to point out that WSOC of those precipitation samples with abnormally high  $\text{Ca}^{2+}$  was mainly influenced by dust. Although  $\text{Ca}^{2+}$  is mainly contributed from dust (Morales-Baquero et al., 2013; Pulido-Villena et al., 2006)

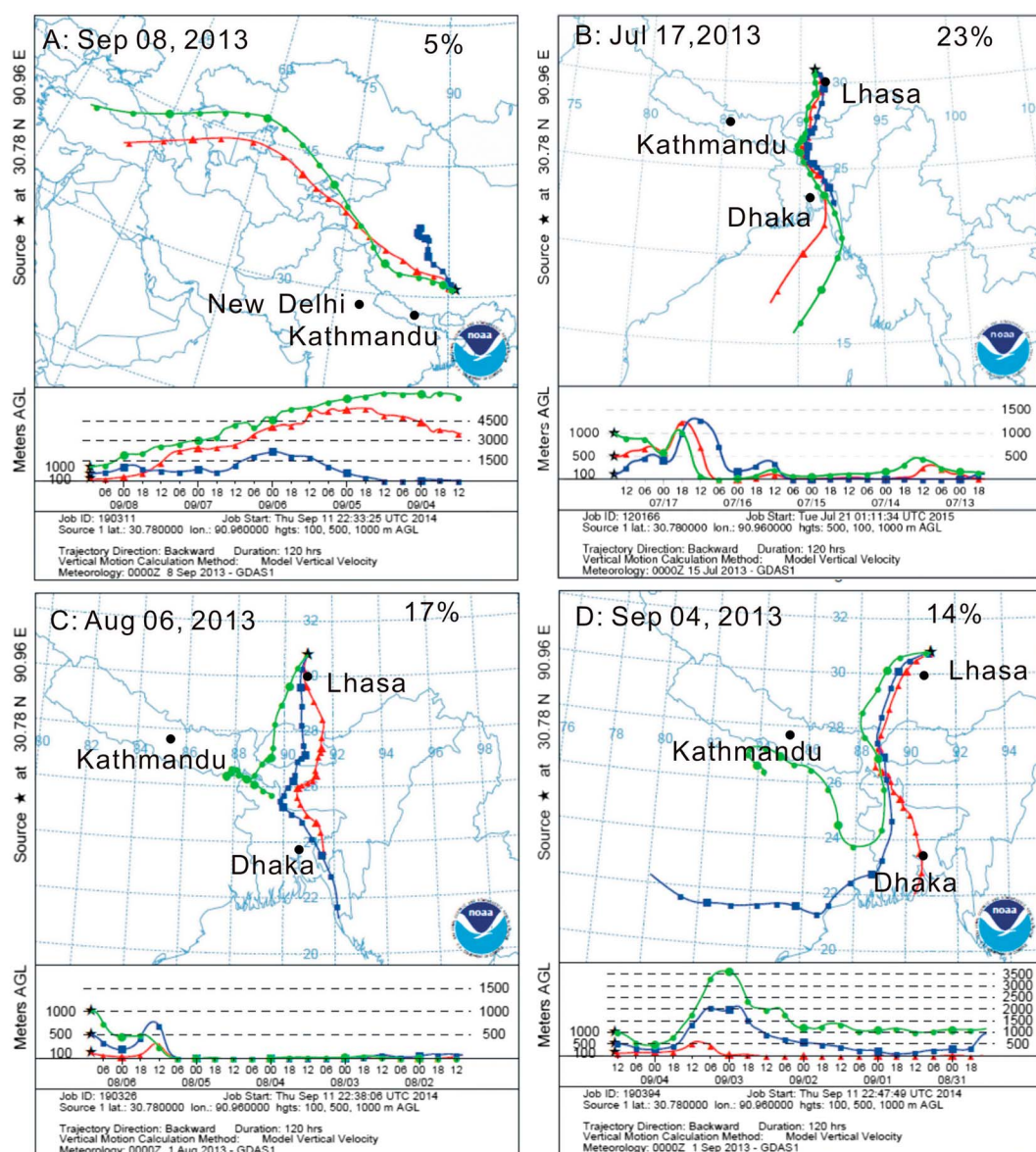


**Figure 5.** Hybrid Single-Particle Lagrangian Integrated Trajectory model backward air mass trajectories and fossil combustion contribution for the (a–d) four typical precipitation events at Nam Co. AGL = above ground level (<http://www.arl.noaa.gov/ready/hysplit4.html>).

and the Taklimakan Desert is located at the north side of study area, it is local sourced dust of the TP that mainly influence  $\text{Ca}^{2+}$  in precipitation at Nam Co station (Li et al., 2012).

In addition, the  $\delta^{13}\text{C}$  signature of organic carbon also provides evidence about its source. The  $\delta^{13}\text{C}$  of organic carbon in soil samples collected from the TP was  $-25.4 \pm 0.6\text{‰}$  (Table S3), similar to those of DOC from Tibetan river water ( $-25.1\text{--}25.8\text{‰}$ ; Qu et al., 2017) and depleted relative to Nam Co WSOC ( $\delta^{13}\text{C} = -21 \pm 3\text{‰}$ ; Table 1), providing further evidence that Nam Co WSOC was not derived from local soils. Enrichment of organic carbon in  $^{13}\text{C}$  can occur in the atmosphere due to both aging processes (Narukawa et al., 1999) and photochemical reactions (Miller & Zepp, 1995; Mladenov, Alados-Arboledas, et al., 2011) altering the original source  $\delta^{13}\text{C}$  signature of organic carbon. Nam Co WSOC enriched in  $^{13}\text{C}$  compared to urban WSOC (Table 1), implying Nam Co WSOC is either derived from a  $^{13}\text{C}$  enriched organic carbon source or has experienced considerable aging during atmospheric transport. As the time available for aging increases with the

distance an air mass travels, the latter would suggest that the organic carbon deposited at Nam Co is sourced in regions distant from the TP.

#### 4.3. Source Regions of Fossil Fuel Combustion-Derived WSOC to Nam Co

The WSOC,  $\text{Ca}^{2+}$ ,  $\text{NO}_3^-$ ,  $\delta^{13}\text{C}$ , and radiocarbon data above imply that Nam Co WSOC is influenced by distant, fossil fuel combustion sources. The geographical source of fossil carbon to WSOC at Nam Co was assessed by back trajectory analysis (Rolph, 2015). This method has been used to determine air mass sources and their influence on aerosols and precipitation on the TP, showing that pollutants were mainly transported from South Asia (C. Li, Bosch, et al., 2016; Liu et al., 2015). In the current study, we further determined the sources of the air masses that corresponded to the seven Nam Co precipitation events for which  $\Delta^{14}\text{C}$ -WSOC was determined.

Among the seven precipitation events, WSOC  $f_{\text{fossil}}$  was the lowest on 8 September 2013 (5%; Table 1). The low-level (500 m AGL) air mass for this precipitation event was transported exclusively from the western TP, a region with few residents and minimal fossil combustion (Figure 5a). Correspondingly, air masses at other altitudes (100 and 1,000 m AGL) derived from the distant Middle East, presumably leading to inefficient transport of pollutants because of long distance transport. Therefore, WSOC for this precipitation event was presumably predominantly sourced from biogenic and biomass burning derived components produced on the TP.

The precipitation events with older WSOC at Nam Co occurred when air masses were transported from South Asia (Figures 5b and 5d). WSOC collected from events during the monsoon (17 July and 6 August 2013) may have been affected by emissions from Lhasa given that low altitude air masses passed over Lhasa before reaching Nam Co (Figures 5b and 5c). Lhasa is the largest city on the TP and only around 150 km from Nam Co (Figure 1). Contribution of fossil fuel combustion to black carbon of Lhasa's atmosphere can be as high as that of Beijing (C. Li, Chen, Kang, Yan, Hu, et al., 2016), resulting in air pollution that influences the  $\Delta^{14}\text{C}$  of WSOC in local precipitation (C. Li, Yan, Kang, Chen, Qu, et al., 2016).

Air masses associated with the four precipitation events with radiocarbon-depleted WSOC during the non-monsoon period were also transported from South Asia (Figure S4). Although westerlies dominate the TP during nonmonsoon period, air masses derived from South Asia can penetrate into the TP occasionally, especially in April and May before the outbreak of the Indian monsoon (Luthi et al., 2015). These air mass trajectories are normally wet, warm, and more likely to lead to precipitation than the more common westerlies. For instance, most precipitation events at Nam Co during 2011–2012 were seeded by air masses transported from South Asia (Liu et al., 2015). Therefore, both the incidence of precipitation events and the delivery of fossil fuel-derived organics to the TP are greater when air masses are sourced over South Asia, making these events the main drivers of annual fossil fuel-derived WSOC fluxes to Nam Co. Conversely, air masses associated with westerlies result in lower fossil fuel contributions to WSOC within any precipitation that does occur. Only one precipitation seeded by an air mass transported by westerly winds was captured. More precipitation events should be studied in the future to better test the above conclusions. Nevertheless, the air masses of the other six Nam Co precipitation events derived from South Asia provide strong evidence that fossil fuel combustion-derived organics from South Asia are transported into the TP during both monsoon and nonmonsoon periods.

## 5. Conclusions

Carbon isotopic compositions of WSOC at Nam Co, a typical remote area of the TP, supplemented with FT-ICR MS, major ions, and air mass trajectory data, indicate that long-range transport of fossil fuel combustion sourced organic carbon influence the quantity of WSOC delivered to Nam Co. Previous studies on the TP also support this conclusion based upon Community Atmosphere Model (R. Zhang, Wang, et al., 2015) and  $\Delta^{14}\text{C}$  of black carbon (C. Li, Bosch, et al., 2016). This study further shows that about 15% of the WSOC at Nam Co region and glacier regions comes from fossil fuel combustion. Correspondingly, the other WSOC are derived from multiple modern sources such as biomass mass burning, various gaseous precursors, and organic gases. The exact sources need to be further investigated in the future.

The fossil signal of WSOC in rain and snow falling onto the remote TP, the rooftop of the world, demonstrates the far-reaching consequences of industrial activity and the interconnectivity of the global anthropogenic



and natural biogeochemical cycles. The WSOC deposited to glacier ecosystems in Alaska and on the TP has been shown to be both biolabile and contains significant inputs from fossil fuel combustion-derived carbon (Spencer et al., 2014; Stubbins et al., 2012). Although the biolability of WSOC delivered to the TP has yet to be directly addressed, it may also be biolabile. Thus, the atmospheric chemistry, rain and snow water chemistry, and the functioning of snow and ice covered ecosystems on the remote TP are likely being modified by long-range transport and deposition of anthropogenic organic carbon.

## Acknowledgments

This study was supported by the Strategic Priority Research Program of Chinese Academy of Chinese Sciences, Pan-Third Pole Environment Study for a Green Silk Road (Pan-TPE) (XDA20040501), the National Nature Science Foundation of China (41675130, 41721091 and 41630754), State Key Laboratory of Cryospheric Science (SKLCS-ZZ-2017), Chinese Academy of Sciences (QYZDY-SSW-DQC039), China Postdoctoral Science Foundation (2016 M602897), and the U.S. National Science Foundation (DEB-1146161 and DEB-1145313). The data used in the paper can be found in Tables S1–S3 of the supporting information file and the excel file (2017JD028181-Dataset). The authors express their thanks to Lan Mu, Xiluo, and Duoie Ciren at Nam Co Station for assistance in collecting samples.

## References

- Antony, R., Grannas, A. M., Willoughby, A. S., Sleighter, R. L., Thamban, M., & Hatcher, P. G. (2014). Origin and sources of dissolved organic matter in snow on the East Antarctic ice sheet. *Environmental Science & Technology*, 48(11), 6151–6159. <https://doi.org/10.1021/es405246a>
- Avery, G., Willey, J., & Kieber, R. (2006). Carbon isotopic characterization of dissolved organic carbon in rainwater: Terrestrial and marine influences. *Atmospheric Environment*, 40(39), 7539–7545. <https://doi.org/10.1016/j.atmosenv.2006.07.014>
- Avery, G. B., Biswas, K. F., Mead, R., Southwell, M., Willey, J. D., Kieber, R. J., & Mullaugh, K. M. (2013). Carbon isotopic characterization of hydrophobic dissolved organic carbon in rainwater. *Atmospheric Environment*, 68, 230–234. <https://doi.org/10.1016/j.atmosenv.2012.11.054>
- Barker, J. D., Dubnick, A., Lyons, W. B., & Chin, Y. P. (2013). Changes in dissolved organic matter (DOM) fluorescence in proglacial Antarctic streams. *Arctic Antarctic and Alpine Research*, 45(3), 305–317. <https://doi.org/10.1657/1938-4246-45.3.305>
- Chen, B., Andersson, A., Lee, M., Kirillova, E. N., Xiao, Q., Kruså, M., et al. (2013). Source forensics of black carbon aerosols from China. *Environmental Science & Technology*, 47(16), 9102–9108. <https://doi.org/10.1021/es401599r>
- Chen, P., Kang, S., Li, C., Rupakheti, M., Yan, F., Li, Q., et al. (2015). Characteristics and sources of polycyclic aromatic hydrocarbons in atmospheric aerosols in the Kathmandu Valley, Nepal. *Science of the Total Environment*, 538, 86–92. <https://doi.org/10.1016/j.scitotenv.2015.08.006>
- Decesari, S., Facchini, M. C., Fuzzi, S., & Tagliavini, E. (2000). Characterization of water-soluble organic compounds in atmospheric aerosol: A new approach. *Journal of Geophysical Research*, 105, 1481–1489. <https://doi.org/10.1029/1999JD900950>
- Dittmar, T., Koch, B., Hertkorn, N., & Kattner, G. (2008). A simple and efficient method for the solid-phase extraction of dissolved organic matter (SPE-DOM) from seawater. *Limnology and Oceanography: Methods*, 6(6), 230–235. <https://doi.org/10.4319/lom.2008.6.230>
- Drever, J. I. (1982). *The geochemistry of natural waters*. Englewood Cliffs, NJ: Prentice-Hall Englewood Cliffs.
- Duarte, R. M., & Duarte, A. C. (2011). A critical review of advanced analytical techniques for water-soluble organic matter from atmospheric aerosols. *TrAC Trends in Analytical Chemistry*, 30(10), 1659–1671. <https://doi.org/10.1016/j.trac.2011.04.020>
- Duarte, R. M. B. O., Santos, E. B. H., Pio, C. A., & Duarte, A. C. (2007). Comparison of structural features of water-soluble organic matter from atmospheric aerosols with those of aquatic humic substances. *Atmospheric Environment*, 41(37), 8100–8113. <https://doi.org/10.1016/j.atmosenv.2007.06.034>
- Fellman, J. B., Hood, E., Raymond, P. A., Stubbins, A., & Spencer, R. G. M. (2015). Spatial variation in the origin of dissolved organic carbon in snow on the Juneau Icefield, Southeast Alaska. *Environmental Science & Technology*, 49(19), 11492–11499. <https://doi.org/10.1021/acs.est.5b02685>
- Grannas, A. M., Shepson, P. B., & Filley, T. R. (2004). Photochemistry and nature of organic matter in Arctic and Antarctic snow. *Global Biogeochemical Cycles*, 18, GB1006. <https://doi.org/10.1029/2003GB002133>
- Graven, H. D. (2015). Impact of fossil fuel emissions on atmospheric radiocarbon and various applications of radiocarbon over this century. *Proceedings of the National Academy of Sciences*, 112(31), 9542–9545. <https://doi.org/10.1073/pnas.1504467112>
- Gustafsson, Ö., Kruså, M., Zencak, Z., Sheesley, R. J., Granat, L., Engström, E., et al. (2009). Brown clouds over South Asia: Biomass or fossil fuel combustion? *Science*, 323(5913), 495–498. <https://doi.org/10.1126/science.1164857>
- Hood, E., Battin, T. J., Fellman, J., O'Neil, S., & Spencer, R. G. M. (2015). Storage and release of organic carbon from glaciers and ice sheets. *Nature Geoscience*, 8(2), 91–96. <https://doi.org/10.1038/ngeo2331>
- Hood, E., Fellman, J., Spencer, R. G. M., Hernes, P. J., Edwards, R., D'Amore, D., & Scott, D. (2009). Glaciers as a source of ancient and labile organic matter to the marine environment. *Nature*, 462(7276), 1044–1047. <https://doi.org/10.1038/nature08580>
- Huang, J., Kang, S., Shen, C., Cong, Z., Liu, K., Wang, W., & Liu, L. (2010). Seasonal variations and sources of ambient fossil and biogenic-derived carbonaceous aerosols based on <sup>14</sup>C measurements in Lhasa, Tibet. *Atmospheric Research*, 96(4), 553–559. <https://doi.org/10.1016/j.atmosres.2010.01.003>
- Ji, Z., Kang, S., Cong, Z., Zhang, Q., & Yao, T. (2015). Simulation of carbonaceous aerosols over the Third Pole and adjacent regions: Distribution, transportation, deposition, and climatic effects. *Climate Dynamics*, 45(9–10), 2831–2846. <https://doi.org/10.1007/s00382-015-2509-1>
- Kang, S., Chen, P., Li, C., Liu, B., & Cong, Z. (2016). Atmospheric aerosol elements over the inland Tibetan Plateau: Concentration, seasonality, and transport. *Aerosol and Air Quality Research*, 16(3), 789–800. <https://doi.org/10.4209/aaqr.2015.05.0307>
- Kim, S., Kaplan, L. A., Benner, R., & Hatcher, P. G. (2004). Hydrogen-deficient molecules in natural riverine water samples—Evidence for the existence of black carbon in DOM. *Marine Chemistry*, 92(1–4), 225–234. <https://doi.org/10.1016/j.marchem.2004.06.042>
- Kirillova, E. N., Andersson, A., Sheesley, R. J., Kruså, M., Praveen, P. S., Budhavant, K., et al. (2013). <sup>13</sup>C- and <sup>14</sup>C-based study of sources and atmospheric processing of water-soluble organic carbon (WSOC) in South Asian aerosols. *Journal of Geophysical Research: Atmospheres*, 118, 614–626. <https://doi.org/10.1002/jgrd.50130>
- Koch, B. P., & Dittmar, T. (2006). From mass to structure: An aromaticity index for high-resolution mass data of natural organic matter. *Rapid Communications in Mass Spectrometry*, 20(5), 926–932. <https://doi.org/10.1002/rcm.2386>
- Koch, B. P., Dittmar, T., Witt, M., & Kattner, G. (2007). Fundamentals of molecular formula assignment to ultrahigh resolution mass data of natural organic matter. *Analytical Chemistry*, 79(4), 1758–1763. <https://doi.org/10.1021/ac061949s>
- Legrand, M., Preunkert, S., Jourdain, B., Guilhermet, J., Alekhina, I., & Petit, J. R. (2013). Water-soluble organic carbon in snow and ice deposited at Alpine, Greenland, and Antarctic sites: A critical review of available data and their atmospheric relevance. *Climate of the Past*, 9(5), 2195–2211. <https://doi.org/10.5194/cp-9-2195-2013>
- Legrand, M., Preunkert, S., Schock, M., Cerqueira, M., Kasper-Giebl, A., Afonso, J., et al. (2007). Major 20th century changes of carbonaceous aerosol components (EC, WinOC, DOC, HULIS, carboxylic acids, and cellulose) derived from Alpine ice cores. *Journal of Geophysical Research*, 112, D23S11. <https://doi.org/10.1029/2006JD008080>

- Li, C., Bosch, C., Kang, S., Andersson, A., Chen, P., Zhang, Q., et al. (2016). Sources of black carbon to the Himalayan–Tibetan Plateau glaciers. *Nature Communications*, 7, 12,574. <https://doi.org/10.1038/ncomms12574>
- Li, C., Chen, P., Kang, S., Yan, F., Hu, Z., Qu, B., & Sillanpää, M. (2016). Concentrations and light absorption characteristics of carbonaceous aerosol in PM<sub>2.5</sub> and PM<sub>10</sub> of Lhasa city, the Tibetan Plateau. *Atmospheric Environment*, 127, 340–346. <https://doi.org/10.1016/j.atmosenv.2015.12.059>
- Li, C., Chen, P., Kang, S., Yan, F., Li, X., Qu, B., & Sillanpää, M. (2016). Carbonaceous matter deposition in the high glacial regions of the Tibetan Plateau. *Atmospheric Environment*, 141, 203–208. <https://doi.org/10.1016/j.atmosenv.2016.06.064>
- Li, C., Kang, S., Zhang, Q., & Gao, S. (2012). Geochemical evidence on the source regions of Tibetan Plateau dusts during non-monsoon period in 2008/09. *Atmospheric Environment*, 59, 382–388. <https://doi.org/10.1016/j.atmosenv.2012.06.006>
- Li, C., Kang, S., Zhang, Q., & Kaspari, S. (2007). Major ionic composition of precipitation in the Nam Co region, central Tibetan Plateau. *Atmospheric Research*, 85(3–4), 351–360. <https://doi.org/10.1016/j.atmosres.2007.02.006>
- Li, C., Yan, F., Kang, S., Chen, P., Hu, Z., Han, X., et al. (2017). Deposition and light absorption characteristics of precipitation dissolved organic carbon (DOC) at three remote stations in the Himalayas and Tibetan Plateau, China. *Science of the Total Environment*, 605, 1039–1046. <https://doi.org/10.1016/j.scitotenv.2017.06.232>
- Li, C., Yan, F., Kang, S., Chen, P., Qu, B., Hu, Z., & Sillanpää, M. (2016). Concentration, sources, and flux of dissolved organic carbon of precipitation at Lhasa city, the Tibetan Plateau. *Environmental Science and Pollution Research*, 23(13), 12,915–12,921. <https://doi.org/10.1007/s11356-016-6455-1>
- Li, X., Kang, S., He, X., Qu, B., Tripathi, L., Jing, Z., et al. (2017). Light-absorbing impurities accelerate glacier melt in the Central Tibetan Plateau. *Science of the Total Environment*, 587, 482–490. <https://doi.org/10.1016/j.scitotenv.2017.02.169>
- Liu, Y. W., Xu, R., Wang, Y. S., Pan, Y. P., & Piao, S. L. (2015). Wet deposition of atmospheric inorganic nitrogen at five remote sites in the Tibetan Plateau. *Atmospheric Chemistry and Physics*, 15(20), 11,683–11,700. <https://doi.org/10.5194/acp-15-11683-2015>
- Lu, H. Y., Wu, N. Q., Gu, Z. Y., Guo, Z. T., Wang, L., Wu, H. B., et al. (2004). Distribution of carbon isotope composition of modern soils on the Qinghai-Tibetan Plateau. *Biogeochemistry*, 70(2), 273–297.
- Luthi, Z. L., Skerlak, B., Kim, S. W., Lauer, A., Mues, A., Rupakheti, M., & Kang, S. (2015). Atmospheric brown clouds reach the Tibetan Plateau by crossing the Himalayas. *Atmospheric Chemistry and Physics*, 15(11), 6007–6021. <https://doi.org/10.5194/acp-15-6007-2015>
- May, B., Wagenbach, D., Hoffmann, H., Legrand, M., Preunkert, S., & Steier, P. (2013). Constraints on the major sources of dissolved organic carbon in Alpine ice cores from radiocarbon analysis over the bomb-peak period. *Journal of Geophysical Research: Atmospheres*, 118, 3319–3327. <https://doi.org/10.1002/jgrd.50200>
- Miller, W. L., & Zepp, R. G. (1995). Photochemical production of dissolved inorganic carbon from terrestrial organic matter: Significance to the oceanic organic carbon cycle. *Geophysical Research Letters*, 22, 417–420. <https://doi.org/10.1029/94GL03344>
- Mladenov, N., Alados-Arboledas, L., Olmo, F. J., Lyamani, H., Delgado, A., Molina, A., & Reche, I. (2011). Applications of optical spectroscopy and stable isotope analyses to organic aerosol source discrimination in an urban area. *Atmospheric Environment*, 45(11), 1960–1969. <https://doi.org/10.1016/j.atmosenv.2011.01.029>
- Mladenov, N., Pulido-Villena, E., Morales-Baquero, R., Ortega-Retuerta, E., Sommaruga, R., & Reche, I. (2008). Spatiotemporal drivers of dissolved organic matter in high alpine lakes: Role of Saharan dust inputs and bacterial activity. *Journal of Geophysical Research*, 113, G00D01. <https://doi.org/10.1029/2008JG000699>
- Mladenov, N., Sommaruga, R., Morales-Baquero, R., Laurion, I., Camarero, L., Dieguez, M. C., et al. (2011). Dust inputs and bacteria influence dissolved organic matter in clear alpine lakes. *Nature Communications*, 2, 405. <https://doi.org/10.1038/ncomms1411>
- Mopper, K., Stubbins, A., Ritchie, J. D., Bialk, H. M., & Hatcher, P. G. (2007). Advanced instrumental approaches for characterization of marine dissolved organic matter: Extraction techniques, mass spectrometry, and nuclear magnetic resonance spectroscopy. *Chemical Reviews*, 107(2), 419–442. <https://doi.org/10.1021/cr050359b>
- Morales-Baquero, R., Pulido-Villena, E., & Reche, I. (2013). Chemical signature of Saharan dust on dry and wet atmospheric deposition in the south-western Mediterranean region. *Tellus Series B: Chemical and Physical Meteorology*, 65(1), 18720. <https://doi.org/10.3402/tellusb.v65i0.18720>
- Narukawa, M., Kawamura, K., Takeuchi, N., & Nakajima, T. (1999). Distribution of dicarboxylic acids and carbon isotopic compositions in aerosols from 1997 Indonesian forest fires. *Geophysical Research Letters*, 26, 3101–3104. <https://doi.org/10.1029/1999GL010810>
- Pan, Y., Wang, Y., Xin, J., Tang, G., Song, T., Wang, Y., et al. (2010). Study on dissolved organic carbon in precipitation in Northern China. *Atmospheric Environment*, 44(19), 2350–2357. <https://doi.org/10.1016/j.atmosenv.2010.03.033>
- Pulido-Villena, E., Reche, I., & Morales-Baquero, R. (2006). Significance of atmospheric inputs of calcium over the southwestern Mediterranean region: High mountain lakes as tools for detection. *Global Biogeochemical Cycles*, 20, GB2012. <https://doi.org/10.1029/2005GB002662>
- Qian, Y., Flanner, M. G., Leung, L. R., & Wang, W. (2011). Sensitivity studies on the impacts of Tibetan Plateau snowpack pollution on the Asian hydrological cycle and monsoon climate. *Atmospheric Chemistry and Physics*, 11(5), 1929–1948. <https://doi.org/10.5194/acp-11-1929-2011>
- Qu, B., Sillanpää, M., Li, C., Kang, S., Stubbins, A., Yan, F., et al. (2017). Aged dissolved organic carbon exported from rivers of the Tibetan Plateau. *PLoS One*, 12(5). <https://doi.org/10.1371/journal.pone.0178166>
- Ramanathan, V., & Carmichael, G. (2008). Global and regional climate changes due to black carbon. *Nature Geoscience*, 1(4), 221–227. <https://doi.org/10.1038/ngeo156>
- Raymond, P. A. (2005). The composition and transport of organic carbon in rainfall: Insights from the natural (<sup>13</sup>C and <sup>14</sup>C) isotopes of carbon. *Geophysical Research Letters*, 32, L14402. <https://doi.org/10.1029/2005GL022879>
- Raymond, P. A., Bauer, J. E., Caraco, N. F., Cole, J. J., Longworth, B., & Petsch, S. T. (2004). Controls on the variability of organic matter and dissolved inorganic carbon ages in northeast US rivers. *Marine Chemistry*, 92(1–4), 353–366. <https://doi.org/10.1016/j.marchem.2004.06.036>
- Raymond, P. A., McClelland, J. W., Holmes, R. M., Zhulidov, A. V., Mull, K., Peterson, B. J., et al. (2007). Flux and age of dissolved organic carbon exported to the Arctic Ocean: A carbon isotopic study of the five largest arctic rivers. *Global Biogeochemical Cycles*, 21, GB4011. <https://doi.org/10.1029/2007GB002934>
- Rolph, G. D. (2015). Real-time Environmental Applications and Display sYstem (READY) Website (<http://ready.arl.noaa.gov>), NOAA Air Resources Laboratory, Silver Spring, MD.
- Singer, G. A., Fasching, C., Wilhelm, L., Niggemann, J., Steier, P., Dittmar, T., & Battin, T. J. (2012). Biogeochemically diverse organic matter in Alpine glaciers and its downstream fate. *Nature Geoscience*, 5(10), 710–714. <https://doi.org/10.1038/ngeo1581>
- Spencer, R. G. M., Guo, W., Raymond, P. A., Dittmar, T., Hood, E., Fellman, J., & Stubbins, A. (2014). Source and biolability of ancient dissolved organic matter in glacier and lake ecosystems on the Tibetan Plateau. *Geochimica et Cosmochimica Acta*, 142, 64–74. <https://doi.org/10.1016/j.gca.2014.08.006>

- Stubbins, A., & Dittmar, T. (2012). Low volume quantification of dissolved organic carbon and dissolved nitrogen. *Limnology and Oceanography: Methods*, 10(5), 347–352. <https://doi.org/10.4319/lom.2012.10.347>
- Stubbins, A., Hood, E., Raymond, P. A., Aiken, G. R., Sleighter, R. L., Hernes, P. J., et al. (2012). Anthropogenic aerosols as a source of ancient dissolved organic matter in glaciers. *Nature Geoscience*, 5(3), 198–201. <https://doi.org/10.1038/ngeo1403>
- Stubbins, A., Lapierre, J. F., Berggren, M., Prairie, Y. T., Dittmar, T., & del Giorgio, P. A. (2014). What's in an EEM? Molecular signatures associated with dissolved organic fluorescence in boreal Canada. *Environmental Science & Technology*, 48(18), 10,598–10,606. <https://doi.org/10.1021/es502086e>
- Stubbins, A., Spencer, R. G. M., Chen, H. M., Hatcher, P. G., Mopper, K., Hernes, P. J., et al. (2010). Illuminated darkness: Molecular signatures of Congo River dissolved organic matter and its photochemical alteration as revealed by ultrahigh precision mass spectrometry. *Limnology and Oceanography*, 55(4), 1467–1477. <https://doi.org/10.4319/lo.2010.55.4.1467>
- Twickler, M. S., Spencer, M. J., Lyons, W. B., & Mayewski, P. A. (1986). Measurement of organic carbon in polar snow samples. *Nature*, 320(6058), 156–158. <https://doi.org/10.1038/320156a0>
- Willey, J. D., Kieber, R. J., Eyman, M. S., & Avery Jr, G. B. (2000). Rainwater dissolved organic carbon: Concentrations and global flux. *Global Biogeochemical Cycles*, 14, 139–148. <https://doi.org/10.1029/1999GB900036>
- Wozniak, A. S., Bauer, J. E., Sleighter, R. L., & Dickhut, R. M. (2008). Molecular characterization of aerosol-derived water soluble organic carbon using ultrahigh resolution electrospray ionization Fourier transform ion cyclotron resonance mass spectrometry. *Atmospheric Chemistry and Physics*, 8(17), 5099–5111. <https://doi.org/10.5194/acp-8-5099-2008>
- Wozniak, A. S., Bauer, J. E., Sleighter, R. L., Dickhut, R. M., & Hatcher, P. G. (2008). Technical note: Molecular characterization of aerosol-derived water soluble organic carbon using ultrahigh resolution electrospray ionization Fourier transform ion cyclotron resonance mass spectrometry. *Atmospheric Chemistry and Physics*, 8(17), 5099–5111. <https://doi.org/10.5194/acp-8-5099-2008>
- Xu, J. Z., Zhang, Q., Li, X. Y., Ge, X. L., Xiao, C. D., Ren, J. W., & Qin, D. H. (2013). Dissolved organic matter and inorganic ions in a central Himalayan glacier—insights into chemical composition and atmospheric sources. *Environmental Science & Technology*, 47(12), 6181–6188. <https://doi.org/10.1021/es4009882>
- Yan, F., Kang, S., Li, C., Zhang, Y., Qin, X., Li, Y., et al. (2016). Concentration, sources and light absorption characteristics of dissolved organic carbon on a medium-sized valley glacier, northern Tibetan Plateau. *The Cryosphere*, 10(6), 2611–2621. <https://doi.org/10.5194/tc-10-2611-2016>
- Yan, G., & Kim, G. (2012). Dissolved organic carbon in the precipitation of Seoul, Korea: Implications for global wet depositional flux of fossil-fuel derived organic carbon. *Atmospheric Environment*, 59, 117–124. <https://doi.org/10.1016/j.atmosenv.2012.05.044>
- Yang, H., Li, Q., & Yu, J. Z. (2003). Comparison of two methods for the determination of water-soluble organic carbon in atmospheric particles. *Atmospheric Environment*, 37(6), 865–870. [https://doi.org/10.1016/S1352-2310\(02\)00953-6](https://doi.org/10.1016/S1352-2310(02)00953-6)
- Zencak, Z., Elmquist, M., & Gustafsson, O. (2007). Quantification and radiocarbon source apportionment of black carbon in atmospheric aerosols using the CTO-375 method. *Atmospheric Environment*, 41(36), 7895–7906. <https://doi.org/10.1016/j.atmosenv.2007.06.006>
- Zhang, R., Wang, H., Qian, Y., Rasch, P. J., Easter, R. C., Ma, P. L., et al. (2015). Quantifying sources, transport, deposition, and radiative forcing of black carbon over the Himalayas and Tibetan Plateau. *Atmospheric Chemistry and Physics*, 15(11), 6205–6223. <https://doi.org/10.5194/acp-15-6205-2015>
- Zhang, Y., Kang, S., Cong, Z., Schmale, J., Sprenger, M., Li, C., et al. (2017). Light-absorbing impurities enhance glacier albedo reduction in the southeastern Tibetan Plateau. *Journal of Geophysical Research: Atmospheres*, 122, 6915–6933. <https://doi.org/10.1002/2016JD026397>
- Zhang, Y.-L., Huang, R.-J., El Haddad, I., Ho, K.-F., Cao, J.-J., Han, Y., et al. (2015). Fossil vs. non-fossil sources of fine carbonaceous aerosols in four Chinese cities during the extreme winter haze episode of 2013. *Atmospheric Chemistry and Physics*, 15(3), 1299–1312. <https://doi.org/10.5194/acp-15-1299-2015>